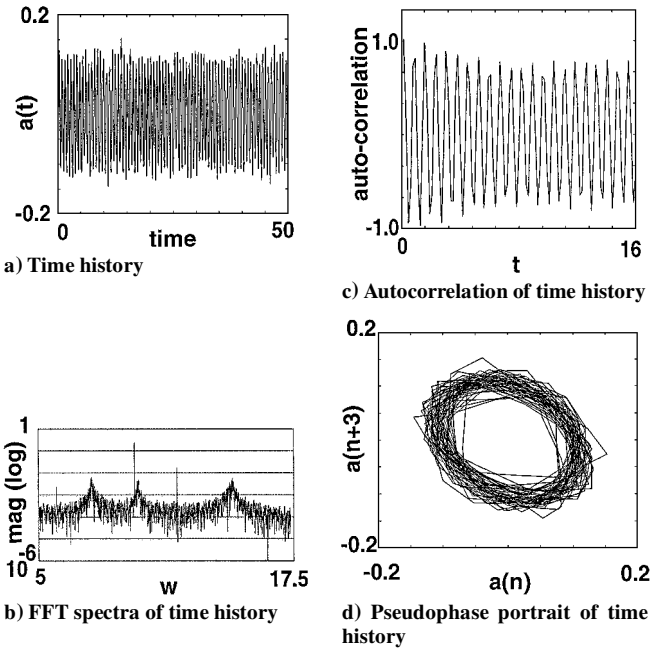

Fig. 3 Periodic response measured from the accelerometer at the tip of the beam in the out-of-plane direction with excitation frequency 9.6875 Hz.

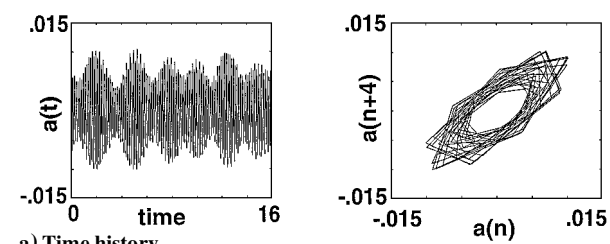

Fig. 4 Amplitude modulated response measured from the accelerometer at the same location as in Fig. 3, with excitation frequency 9.8 Hz.

frequency of the lead/lag mode was found to be 9.82 Hz. Figure 3c is a portion of the autocorrelation of the time history. It shows that noise is not appreciable. The minor loss of correlation indicates that the motion is nearly periodic. One-quarter of the natural orbital period is chosen to get an open pseudophase portrait. Figure 3d is the pseudophase portrait created following the time delay embedding procedure outlined by Broomhead and King.[4] An embedding delay of three was used for this case.

The excitation frequency was then increased to 9.90 Hz. The excitation amplitude was held constant by monitoring the output from the load cell and manually adjusting the input voltage to the exciter. Figure 4a is a time history again recorded from the accelerometer near the free end of the beam in the flapping direction. It clearly shows a beatinglike appearance typical of an amplitude modulated response. The time history in the lead/lag direction (not shown) has a similar appearance. A pseudophase portrait of the response is shown in Fig. 4b using an embedding delay of four. In this case the thickness of the ellipse arises more from the amplitude modulation of the response than from the noise. The amplitude and period of modulation can be approximated by the motion of a point on a torus.[5] A Poincaré section of the response would be more definitive in determining the aperiodicity of the response. However, one could not be constructed in this case because the data were not sampled at a suitable frequency such as an integer multiple of the excitation frequency.

III. Conclusion

A periodic and a limit cycle response of a cantilever beam attached to a rotating body subject to a harmonic excitation has been presented. The experimental measurement of these motions supports a theoretical study that predicts a variety of nonlinear dynamic responses.

Acknowledgments

This work was performed under the auspices of the U.S. Department of Energy by the Lawrence Livermore National Laboratory under Contract W-7405-ENG-48. The support of Jerry Gerich and Robert Langland is greatly appreciated.

References

[1] Murphy, K. D., and Lee, C. L., "The 1:1 Internally Resonant Response of a Cantilever Beam Attached to a Rotating Beam," *Journal of Sound and Vibration*, Vol. 211, No. 2, 1998, pp. 179–194.

[2] Bajaj, A. K., and Johnson, J. M., "Asymptotic Techniques and Complex Dynamics in Weakly Non-Linear Forced Mechanical Systems," *International Journal of Non-Linear Mechanics*, Vol. 25, No. 2/3, 1990, pp. 211–226.

[3] Lee, C. L., Al-Salem, M. F., and Woehrle, T. G., "Natural Frequency Measurements for Rotating Spanwise Uniform Cantilever Beams," *Journal of Applied Mechanics* (submitted for publication).

[4] Broomhead, D. S., and King, G. P., "Extracting Qualitative Dynamics from Experimental Data," *Physica 20D*, 1986, pp. 217–236.

[5] Sethna, P. R., and Bajaj, A. K., "Bifurcations in Dynamical Systems with Internal Resonance," *Journal of Applied Mechanics*, Vol. 45, Dec. 1978, pp. 895–902.

A. Berman
Associate Editor

Application of Parabolized Stability Equations to the Prediction of Jet Instabilities

C. C. Yen* and N. L. Messersmith†
Purdue University, West Lafayette, Indiana 47907-1282

Introduction

CLASSICAL inviscid and quasiparallel linear stability theory (LST) cannot account for the natural divergence of jet flow. Because of an accumulation effect, incomplete upstream information could lead to inaccurate predictions downstream. Crighton and Gaster[1] and Plaschko[2] accounted for the diverging effect by the multiple-scales method; however, this is subject to inherent numerical difficulties when neglecting viscosity. Furthermore, neither method can account for the possible distortion of instability waveforms near the jet exit, which could largely influence downstream instabilities. A newly developed method called *parabolized stability equations* (PSE)[3–6] has been used to analyze the streamwise evolution of instability waves in flows that are highly unidirectional, such as boundary layers and free shear layers. That the PSE analysis is able to fully account for the nature of diverging mean flow and to resolve the evolving instabilities without numerical difficulties as seen in LST has made PSE an alternative tool in dealing with jet instabilities at relatively low computational cost compared with schemes based on direct numerical simulation or large eddy simulation.

PSE for Axisymmetric Flow

Yen and Messersmith[7] provide details of the PSE derivation in cylindrical coordinates for a viscous incompressible circular free jet flow. The mean pressure gradients in the axial and radial directions have been discarded because a free jet is considered. For a diverging mean flow, the solution in terms of LST is not strictly justified because the coefficients of the linearized stability equations depend weakly on the axial location z. Both the amplitude function and wave number exhibit streamwise variation due to the

Received May 30, 1997; revision received April 5, 1998; accepted for publication April 17, 1998.

*Graduate Research Assistant, School of Aeronautics and Astronautics.

†Assistant Professor, School of Aeronautics and Astronautics; currently Project Engineer, Nozzle Technology, Pratt and Whitney, M/S 731-02, P.O. Box 109600, West Palm Beach, FL 33410-9600. Senior Member AIAA.

nonparallel mean flow. Following procedures similar to those employed by Herbert[8] for two-dimensional boundary-layer flows, we retain the decomposition of the solution vector $\boldsymbol{q}' = [u', v', w', p']^T$ into an amplitude function $\boldsymbol{q} = [u, v, w, p]^T$ and a wave function X and write the disturbances in the form

$$\boldsymbol{q}'(r, \phi, z, t) = \boldsymbol{q}(r, z)X(z, \phi, t) \tag{1a}$$

$$X = \exp\{i[-\omega t + n\phi + \eta(z)]\}, \qquad \eta_z = \alpha(z) \tag{1b}$$

where ω is the real angular frequency, t is the time, the integer n is the azimuthal instability mode, and $\alpha(z)$ is the streamwise varying complex wave number.

The nondimensionalized differential equations for the instability wave amplitudes are

$$Du + (u/r) + (inv/r) + i\alpha w + w_z = 0 \tag{2a}$$

$$\begin{aligned}&(-(1/Re)\{D^2 - [\alpha^2 + (n^2/r^2)]\}u + i[\alpha W - \omega + (nV/r)]u \\ &\quad + [(1/r^2Re) - (D/rRe)]u + [(2in/r^2Re) \\ &\quad - (2V/r)]v + Dp) + \{DUu + U_z w\} + \{[W - (2i\alpha/Re)]u_z\} \\ &\quad - \{iu\alpha_z/Re\} = u_{zz}/Re\end{aligned} \tag{2b}$$

$$\begin{aligned}&(-(1/Re)\{D^2 - [\alpha^2 + (n^2/r^2)]\}v + i[\alpha W - \omega + (nV/r)]v \\ &\quad + [(V/r) - (2in/r^2Re)]u + [(1/r^2Re) - (D/rRe)]v \\ &\quad + uDV + (inp/r)) + [UDv + (Uv/r) + V_z w] \\ &\quad + \{[W - (2i\alpha/Re)]v_z\} - \{iv\alpha_z/Re\} = v_{zz}/Re\end{aligned} \tag{2c}$$

$$\begin{aligned}&(-(1/Re)\{D^2 - [\alpha^2 + (n^2/r^2)]\}w + i[\alpha W + (nV/r) - \omega]w \\ &\quad - (Dw/rRe) + uDW + i\alpha p) + \{UDw + wW_z\} \\ &\quad + \{[W - (2i\alpha/Re)]w_z + p_z\} - \{iw\alpha_z/Re\} = w_{zz}/Re\end{aligned} \tag{2d}$$

where $D = \partial/\partial r$ and the perturbations are subject to the boundary conditions at $r = 0$,

$$\frac{\partial u}{\partial r} = \frac{\partial v}{\partial r} = 0 \quad \text{for} \quad n = 1, \qquad u = v = 0 \quad \text{for} \quad n \neq 1 \tag{3a}$$

$$\frac{\partial w}{\partial r} = \frac{\partial p}{\partial r} = 0 \quad \text{for} \quad n = 0, \qquad w = p = 0 \quad \text{for} \quad n \neq 0 \tag{3b}$$

and at $r \to \infty$,

$$u, v, w, p \to 0 \tag{3c}$$

There are four groups of terms on the left-hand side of Eqs. (2a–2d). Each group represents a different contribution to the streamwise evolution of instability waves. Similar groupings were also found in the derivation of PSE for two-dimensional boundary layers.[8] The terms in the first group are identical to those appearing in the stability equations for parallel flow, i.e., no streamwise dependency. The second term accounts for the streamwise changes of the mean flow. The third group consists of the streamwise gradients of the amplitude functions $\boldsymbol{q}$. The last group originates from the streamwise changes of the wave number α.

Once an appropriate function for the spatial wave number α is adopted, the streamwise variation of $\boldsymbol{q}'$ is essentially absorbed in the wave function X, whereas the derivatives $\boldsymbol{q}_z$, α_z, $\boldsymbol{q}_{zz}$, and α_{zz} and the products $\boldsymbol{q}_z\alpha_z$ are small. Hence the parabolization is obtained by ignoring the terms on the right-hand sides of Eqs. (2a–2d), leaving an initial-boundary-value problem. The set of resulting parabolized stability equations is alternatively written in a compact form:

$$L\boldsymbol{q} + M\frac{\partial \boldsymbol{q}}{\partial z} + \frac{\mathrm{d}\alpha}{\mathrm{d}z}N\boldsymbol{q} = 0 \tag{4}$$

where the operators L, M, and N act only in r. By inspection, Eq. (4) can be solved by a marching scheme suitable for parabolic partial differential equations. However, the unknown wave number α appearing in the operators L, M, and N makes Eq. (4) ill posed unless an appropriate algorithm is used to update α at each marching step. Because $\boldsymbol{q}$ is a function of both r and z, α also has a radial dependence. This dependence can be eliminated by an integration scheme using

$$\alpha_{\text{new}} = \alpha_{\text{old}} - i\frac{\int_\Omega \boldsymbol{q}^*\boldsymbol{q}_z \,\mathrm{d}r}{\int_\Omega |\boldsymbol{q}|^2 \,\mathrm{d}r} \tag{5}$$

where the asterisk denotes the complex conjugate and Ω is the radial domain. In the current study for axisymmetric flow, the constituents of $\boldsymbol{q}$ used to update α in Eq. (5) are composed of perturbation velocity components $[u, v, w]^T$. It is noted that different normalizations are also possible in terms of different constituents of $\boldsymbol{q}$ but lead to different partitions of streamwise dependence between $\alpha(z)$ and $\boldsymbol{q}(r, z)$ in Eq. (1a) (Ref. 9). The overall effect on the physical solution $\boldsymbol{q}'$ is small.[8]

A fourth-order central finite difference method is employed in the radial direction to obtain sufficient spatial resolution within the jet shear layer. The streamwise derivative is approximated by forward finite difference form. The system is solved by iteration using a predictor–corrector approach. In the solution procedure, an iteration sequence begins using $\alpha^0_{j+1} = \alpha_j$, allowing $\boldsymbol{q}^0_{j+1}$ to be found, and then subsequently Eq. (5) is used to update the wave number:

$$\alpha^{m+1}_{j+1} = \alpha^m_{j+1} - \frac{i}{\Delta z_j}\frac{\int_\Omega \left(\boldsymbol{q}^m_{j+1}\right)^* \left(\boldsymbol{q}^m_{j+1} - \boldsymbol{q}_j\right) \mathrm{d}r}{\int_\Omega \left|\boldsymbol{q}^m_{j+1}\right|^2 \mathrm{d}r} \tag{6}$$

where m is the iteration index and j is the streamwise step index.

Results and Discussion

Rather than numerically solving the governing equations for the mean flow, an empirical correlation from Crow and Champagne[10] is used for the computations. In its analytical form, the mean flow profile is expressed as

$$\frac{W(r, z)}{W_j} = \frac{1}{2}\left\{1 + \tanh\left[\frac{1}{4}\frac{R_j}{\theta}\left(\frac{R_j}{r} - \frac{r}{R_j}\right)\right]\right\} \tag{7}$$

where θ is the local momentum thickness and $\theta/R_j = 0.03z/R_j + 0.04$. The physical domain of interest starts at the nozzle exit, or $z = 0$. The corresponding initial conditions are generated in terms of classical linear stability analysis with a quasiparallel flow with $\theta/R_j = 0.02$ in which a step-adaptive, Runge–Kutta integration scheme is involved. This eigensolution is then run through the PSE analysis embedded with the nonparallel mean flow. After sharply decaying transients, the spatial instability of the shear layer at $z = 0$ with $\theta/R_j = 0.04$ is readily found, thereby allowing the diverging flow effect to be fully accounted for in the downstream evolving instabilities.

Preliminary computations of the PSE for jet flow exhibit an unstable marching condition when the marching step size Δz is smaller than $1/\alpha_r$. A similar situation was also observed by Li and Malik[11] for incompressible two-dimensional boundary layers. Malik and Li[12] also showed that neglecting the streamwise perturbation pressure gradient p_z does not introduce any serious error and allows smaller step sizes to be used. This argument is also justified in the current study and, therefore, adopted throughout all computations to obtain better streamwise resolution.

The PSE in cylindrical coordinates was initially compared with the inviscid quasiparallel solution from LST. The PSE was found to closely match the predictions from LST when a parallel flow was used. When the diverging mean flow was inserted, the difference between solutions from PSE and LST became clear. The PSE results also compared favorably to existing experiments and theories. In the prediction of inviscid pressure gain along the center of shear layer, over a range of frequencies and at the first three azithumal numbers, the growth history of perturbation pressures is successfully resolved by the PSE, and the dominant instability modes can be

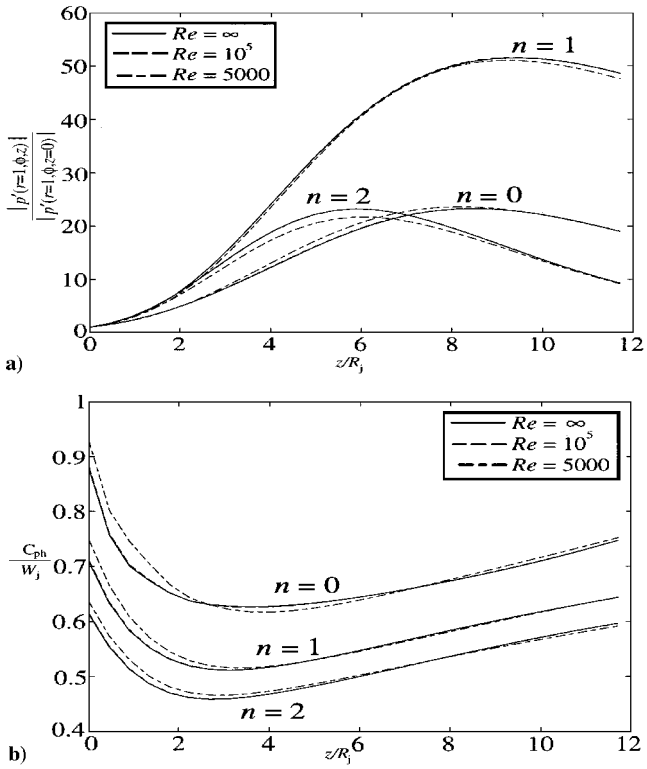

Fig. 1 Influence of Reynolds number on a) pressure gain and b) phase speed in the jet shear layer for $Sr = 0.3$ and $n = 0$, 1, and 2.

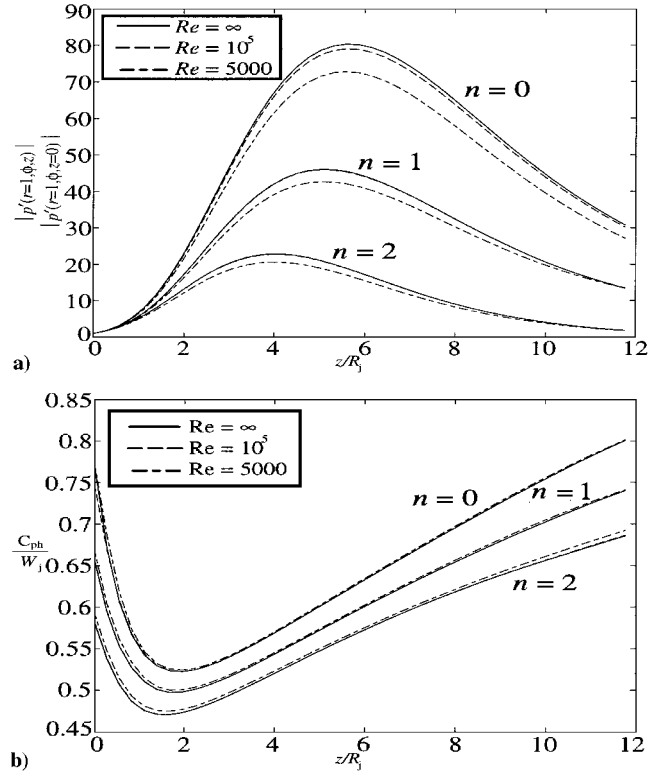

Fig. 2 Influence of Reynolds number on a) pressure gain and b) phase speed in the jet shear layer for $Sr = 0.5$ and $n = 0$, 1, and 2.

readily identified. For the same conditions, the evolution of inviscid phase speeds at the center of the shear layer is also captured. The PSE accurately predicts the streamwise variation and the axial positions where the phase speeds become nondispersive. A more complete discussion can be found in Ref. 7.

The effect of viscosity was also studied. Figures 1 and 2 show the effect of viscosity on the pressure gain and phase speed of perturbation pressure in the center of the jet shear layer for Strouhal numbers of 0.3 and 0.5, respectively. Viscosity is accounted for through the Reynolds number. In general, increasing viscosity (or lowering Reynolds number) stabilizes the disturbance, implying that the inviscid solution will predict the greatest growth rates. Indeed, for $Sr = 0.5$ (Fig. 2), decreasing the Reynolds number shifts slightly upstream and attenuates the peak pressure gain for the first three azimuthal modes. The phase speeds follow expected trends. Similar results were also observed for $Sr = 0.7$.

However, this is not the case for $Sr = 0.3$. As can be seen in Fig. 1 for $n = 0$, $Re = 5 \times 10^3$ is found to produce greater amplification of the disturbance in the middle portion of the jet potential core than $Re = \infty$. For $n = 1$, although the clear emergence of a preferred Reynolds number is not seen, there is a region at $z/R_j = 7$ where Reynolds numbers from 5×10^3 to infinity produce essentially the same pressure gain. These results indicate that instabilities in the developing shear layer can be selectively enhanced at Reynolds numbers that are quite common to many engineering devices and flow processes. Although these results are akin to the results of Morris,[13] there are some important differences. Morris considered three different mean velocity profiles in three different locations to model the diverging flow effect of a natural jet. At each location, though, the numerical solution assumed locally parallel flow, i.e., no streamwise dependence on the wave number. Morris found sensitivity in the local amplification rate to low Reynolds numbers for only $n = 1$ in the far-field jet profile, where it is unclear whether the predicted amplification is actually achieved in the absolute sense or simply due to the normalization of the equations to the decaying centerline velocity. Morris did not observe the same phenomena in the jet near field and the fully developed annular jet mixing region.

In the current study, it is important to note that the observed sensitivity of the disturbance to Reynolds number is not predicted simply at the local level but survives the accumulated influence of the spatially evolving jet flowfield through the jet potential core. In particular, from about $z/R_j = 3$–7 the evolution of the $n = 0$ phase speed for $Re = 5 \times 10^3$ is lower than for the larger Reynolds numbers at $Sr = 0.3$. This is an indication that the local growth rate is more sensitive to the lower Reynolds numbers. When compared with the accumulated pressure gain for the same conditions (Fig. 1), the region of Reynolds number sensitivity is broadened to roughly $z/R_j = 3$–9, illustrating the lingering influence of the spatially developing flowfield captured by the PSE solution. The complex nature of the spatially evolving disturbance and how the local growth rates integrate to form the total pressure gain can be appreciated when considering the $n = 1$ and 2 helical modes of $Sr = 0.3$. The local phase speeds indicate regions of slight Reynolds number sensitivity from $z/R_j = 6$–10 for $n = 1$ and for $z/R_j \geq 8$ when $n = 2$. The pressure gain profiles shown in Fig. 1 do not clearly indicate this effect, but the suggestion can be seen in the nearly identical response in the pressure gain for all Reynolds numbers from $z/R_j = 6$–8 for $n = 1$ and beyond $z/R_j = 10$ for $n = 2$.

Conclusion

The linear PSE have been successfully developed in cylindrical coordinates for the prediction of instabilities in a spatially evolving, incompressible, isothermal, round jet. The results compare quite well with existing theories and experiments. The implementation is easier than the inviscid multiple-scales method, avoiding difficulties in the numerical integration. The PSE analysis is capable of capturing the expected eigensolution over the streamwise domain to the end of the jet potential core where the growing jet shear layer is less capable of supporting the amplified mode. In this sense, the PSE formulation permits the accumulated influence of the developing jet flow to be captured in the solution of not only the local wave number and phase speed but also the integrated gain in the perturbation quantities.

The appearance of a preferred Reynolds number (below the inviscid limit) and Strouhal number combination for the maximum instability amplification represents an intriguing result of the current PSE study. Effects of this nature have been predicted by Morris[13] in a more restricted analysis. The PSE not only captured this sensitivity to viscosity on a local level through the local phase speed but also illustrated the broadening (in a streamwise sense) of the region of sensitivity due to the accumulation effect associated with retaining several streamwise derivative terms in the PSE formulation.

References

[1]Crighton, D. G., and Gaster, M., "Stability of Slowly Diverging Jet Flow," *Journal of Fluid Mechanics*, Vol. 77, 1976, pp. 397–413.

[2]Plaschko, P., "Helical Instabilities of Slowly Divergent Jets," *Journal of Fluid Mechanics*, Vol. 92, Pt. 2, 1979, pp. 209–215.

[3]Herbert, T., and Bertolotti, F. P., "Stability Analysis of Nonparallel Boundary Layers," *Bulletin of the American Physical Society*, Vol. 32, 1987, p. 2079.

[4]Herbert, T., "Boundary-Layer Transition—Analysis and Prediction Revisited," AIAA Paper 91-0737, Jan. 1991.

[5]Chang, C. L., Malik, M. R., Erlebacher, G., and Hussaini, M. Y., "Compressible Stability of Growing Boundary Layers Using Parabolized Stability Equations," AIAA Paper 91-1636, June 1991.

[6]Bertolotti, F. P., and Herbert, T., "Analysis of the Linear Stability of Compressible Boundary Layers Using PSE," *Journal of Theoretical Computational Fluid Mechanics*, Vol. 3, 1991, pp. 117–124.

[7]Yen, C., and Messersmith, N., "Application of Parabolized Stability Equations to the Prediction of Jet Instabilities," AIAA Paper 98-0334, Jan. 1998.

[8]Herbert, T., "Parabolized Stability Equations," AGARD-FDP-VKI Special Course on Progress in Transition Modelling, AGARD-R-793, Von Kármán Inst., Rhode-Saint-Genese, Belgium, 1993.

[9]Bertolotti, F. P., Herbert, T., and Spalart, P. R., "Linear and Nonlinear Stability of the Blasius Boundary Layer," *Journal of Fluid Mechanics*, Vol. 22, 1992, pp. 441–474.

[10]Crow, S. C., and Champagne, F. H., "Orderly Structure in Jet Turbulence," *Journal of Fluid Mechanics*, Vol. 48, Pt. 3, 1971, pp. 547–591.

[11]Li, F., and Malik, M. R., "Step-Size Limitation for Marching Solution Using PSE," 45th Annual Meeting of American Physical Society, Div. of Fluid Dynamics, Tallahassee, FL, 1992.

[12]Malik, M. R., and Li, F., "Transition Studies for Swept Wing Flows Using PSE," AIAA Paper 93-0077, Jan. 1993.

[13]Morris, P. J., "The Spatial Viscous Instability of Axisymmetric Jets," *Journal of Fluid Mechanics*, Vol. 77, Pt. 3, 1976, pp. 511–529.

C. G. Speziale
Associate Editor

Laser Doppler Velocimetry Velocity Bias in Turbulent Open Channel Flow

M. Balakrishnan* and C. L. Dancey†
Virginia Polytechnic Institute and State University, Blacksburg, Virginia 24061-0238

Introduction

THE lack of a universally accepted method to account for velocity bias in individual realization laser Doppler velocimetry (LDV) at all data densities[1] has led to renewed investigations of the practical performance of various postprocessing correction methods in different turbulent flowfields.[2–5] By and large, separated turbulent flows (forward/backward-facing steps, pipe expansions, or body wakes) have been used as the test flow in such studies. However, one- and two-component LDV is commonly used in the investigation of much simpler wall flows, where the impact (or lack of impact) of velocity bias correction on overall mean flow characteristics (such as the friction velocity or the von Kármán constant) is relevant and not easily ascertained from previous investigations.

In the present work the performance of several velocity bias correction methods is evaluated by applying them to a data set obtained with three-component LDV in a fully developed, smooth-walled, open-channel turbulent water flow. In this Note emphasis is placed on the experimental determination of the mean streamwise velocity profile $\langle u \rangle$ (angle brackets denote ensemble averaging), the kinematic Reynolds shear stress profile $\langle u'v' \rangle$ (primes denote fluctuations about the mean, and v is the component normal to the wall), the friction velocity u_*, von Kármán's constant κ, and the intercept of the wall log law. This classical turbulent flow is well suited for this study of velocity bias because it approximates many turbulent flows in its overall characteristics, with turbulence intensities (as measured by the local streamwise rms and mean velocity) ranging from approximately 40% near the wall to a few percent in the core flow. The popular McLaughlin–Tiederman[2] inverse velocity bias correction methods (one, two, and three dimensional), interarrival time weighting (IA), the empirical Gaussian probability density function (PDF) correction method (GPC) of Nakao et al.,[3] and straight ensemble averaging (no correction; NC) are chosen for comparison.

In the most recently reported bias studies by Gould and Loseke[4] and Herrin and Dutton,[5] two-component LDV was employed in the investigation of the shear layer downstream of a low-speed axisymmetric sudden expansion and downstream of a backward-facing step in high-velocity separated flow, respectively. Gould and Loseke concluded that the most effective scheme for reducing velocity bias in the computed mean velocity was the method proposed by Nakao et al.,[3] termed the velocity PDF shape correction technique. The two-dimensional inverse velocity bias method performed well at low turbulence levels and gave some indications of success at higher turbulence levels for high data rates. The data densities[1] were not reported. Herrin and Dutton carried out a similar but more extensive study and concluded that the time-between-data (sample and hold or interarrival time) schemes were very effective, whereas the two-dimensional inverse velocity weighting method compared less favorably, especially at high turbulence intensities. The data density (based on the integral scale of the turbulence) was estimated to be in the low range. The present study includes both the PDF shape correction and IA time methods in addition to others and utilizes a lower turbulence intensity, unseparated, fully developed turbulent flow for the investigation. In the present study the data density (as defined by Edwards[1]) varied between 0.2 and 0.5 for all reported measurement locations, which is in the intermediate range, 0.05–5.0, according to Edwards.

Results and Comparisons

Details of the flume facility, the three-component LDV system, the flow conditions, and the measured velocity field statistics are given elsewhere.[6] For the present investigation, in an effort to make the comparison between bias correction schemes more straightforward, accuracy and precision error contributions (that would obscure the bias correction effects) were overcome by using the same set of measured Doppler frequencies for all bias correction method calculations. That is, although fringe bias, filter bias, particle tracking errors, etc., may be present, exactly the same set of frequency measurements (2048 measurements per point at 80 different positions above the smooth wall) was used for all correction method calculations. Consequently, the variations that are reported between the different methods are entirely and exclusively due to the correction methods themselves. Because the data density was too low for equal time interval sampling to be effective and because no other independent (and bias-free) set of measurements was available (e.g., hot film velocimetry), the three-dimensional McLaughlin–Tiederman inverse velocity correction scheme was chosen as the reference method. This method, at least, utilizes all three components of the measured velocity vector, whereas the other methods either ignore the spanwise component or employ convenient assumptions to account for it.

To demonstrate the presence of bias in the LDV measurements if no correction is employed, the mean streamwise velocity was computed by straight ensemble averaging. The result is shown in Fig. 1, together with the bias predicted according to the theory of Dimotakis.[7] This prediction, derived under the assumption of low transverse (v and w) velocities and low streamwise, $u'/\langle u \rangle$, intensity, is given by

$$\frac{\langle u \rangle_{\text{bias}} - \langle u \rangle}{\langle u \rangle} = \left[\frac{\sigma_u}{\langle u \rangle} \right]^2 \tag{1}$$

Received May 10, 1997; revision received April 16, 1998; accepted for publication April 30, 1998.

*Research Assistant, Department of Mechanical Engineering.

†Assistant Professor, Department of Mechanical Engineering.